

Layer-by-Layer Self-Assembled Graphene Multilayer Films via Covalent Bonds for Supercapacitor Electrodes

Regular Paper

Xianbin Liu¹, Na Wen¹, Xiaoli Wang¹ and Yuying Zheng^{1*}

¹ College of Materials Science and Engineering, Fuzhou University, Fuzhou, China

*Corresponding author(s) E-mail: yyzheng@fzu.edu.cn

Received 12 November 2014; Accepted 08 April 2015

DOI: 10.5772/60596

Licensee InTech. This is an open access article distributed under the terms of the Creative Commons Attribution License (<http://creativecommons.org/licenses/by/3.0>), which permits unrestricted use, distribution, and reproduction in any medium, provided the original work is properly cited.

Abstract

To maximize the utilization of its single-atom thin nature, a facile scheme to fabricate graphene multilayer films via a layer-by-layer self-assembled process was presented. The structure of multilayer films was constructed by covalently bonding graphene oxide (GO) using p-phenylenediamine (PPD) as a covalent cross-linking agent. The assembly process was confirmed to be repeatable and the structure was stable. With the π - π conjugated structure and a large number of spaces in the framework, the graphene multilayer films exhibited excellent electrochemical performance. The uniform ultrathin electrode exhibited a capacitance of 41.71 $\mu\text{F}/\text{cm}^2$ at a discharge current of 0.1 $\mu\text{A}/\text{cm}^2$, and displayed excellent stability of 88.9 % after 1000 charge-discharge cycles.

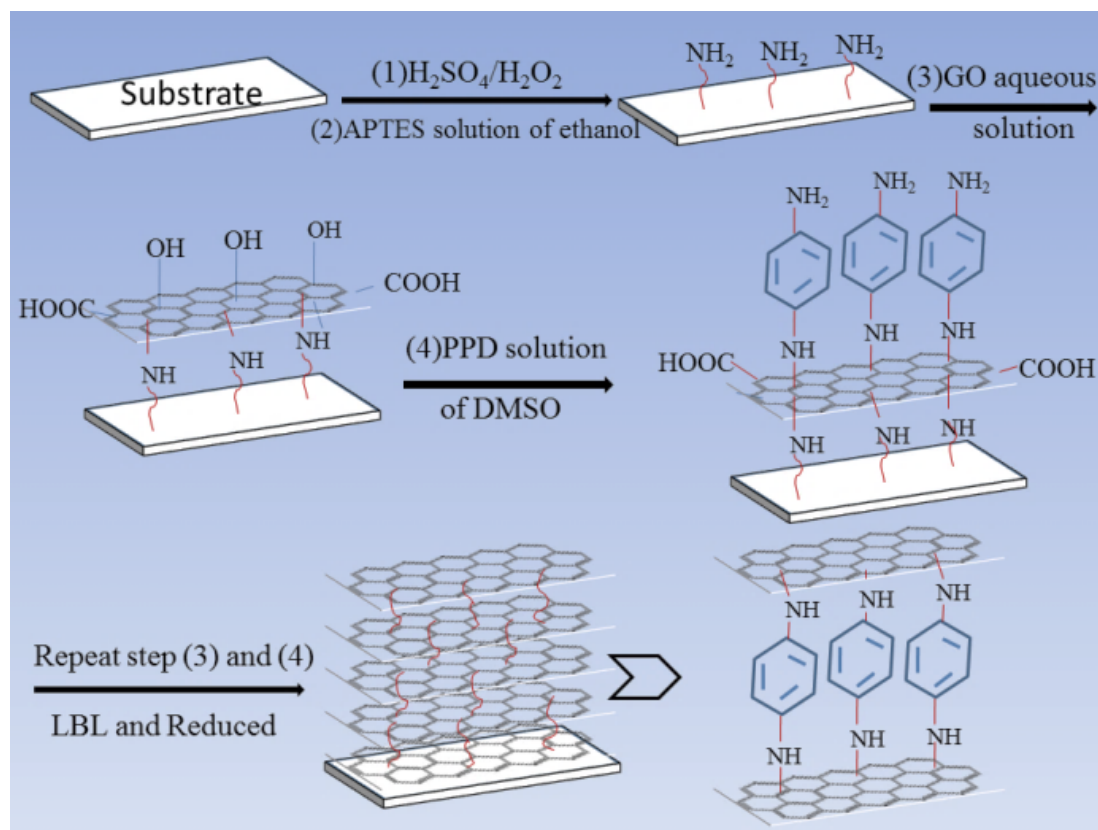
Keywords layer-by-layer self-assembly, covalent bond, graphene, carbon materials, energy storage and conversion

1. Introduction

Supercapacitors have been regarded as an ideal candidate for energy devices, owing to their quick charge times, long life cycles and high power density [1-4]. Considering

energy storage mechanisms, supercapacitors were classified into two types: electrical double layer (EDL) capacitor, and pseudocapacitor. The EDL capacitance was generated by charge adsorption at the electrode/electrolyte interface. Therefore, the structure of electrode materials is crucial for improving EDL capacitance by promoting more electrolyte ion accumulation [5]. Due to the high specific surface area, excellent electronic conductivity and electrochemical stability, carbon-based materials have been widely investigated as supercapacitor electrodes [3, 6, 7].

Graphene, a two-dimensional sp^2 -carbon hexagonal lattice of one-atom thickness, is one of the most attractive materials for supercapacitor electrodes owing to its large theoretical specific surface area of 2675 m^2/g and high electron mobility approaching 20,000 cm^2/Vs [8-10]. Xia et.al [11] reported that the intrinsic capacitance of single-layer graphene is about 21 mF/cm^2 , implying that the theoretical electric double layer capacitance is 550 F/g . However, to date, the realized capacitance was much less than the theoretical value. The loss of capacitance was mainly caused by irreversible agglomeration and re-stacking through π - π interaction [12]. In order to utilize the surface area of each graphene layer to the largest extent, many structures were fabricated, such as curve [12] and wrinkle [13]. On the other hand, incorporating the guest materials



Scheme 1. Schematic illustration of the fabrication procedure of (PPD-rGO)_n multilayer films

that contain conducting polymer [14] or transition metal oxides [15], into graphene nanosheets was beneficial to prevent agglomerating or re-stacking.

Layer-by-layer (LBL) self-assembly, as one of most efficient techniques that could construct well-ordered lamellar nano-architectures, has attracted great attention [16-19]. Most self-assembly processes were based on electrostatic interaction, hydrogen bonds, electrochemistry, and so on [20, 21]. LBL self-assembly via covalent bonds driven by step-by-step reactions, which could achieve the preparation of robust multilayer films, has been less reported. Here, we demonstrated that ultrathin graphene films could be prepared by an LBL covalently assembled method. Utilizing the ring-opening reaction [22], the graphene oxide (GO) nanosheets were jointed with PPD as the bridge. The PPD with a benzene ring not only serves as carriers for the controllable space, but also provides a path for the electronic transmission. As a result, the uniform multilayer films exhibited excellent capacitance property and cycling stability.

2. Experimental Section

Graphite power (300 mesh, 99.95%) was supplied by the Institute of Shenghua (Changsha, China); 3-Aminopropyl triethoxysilane (ATPES, 99%) was obtained from Aladdin (Shanghai, China). All other reagents were purchased from Sinopharm Chemical Reagent Company (Shanghai, China). The substrates, silicon wafers (10×10mm²), quartz

glass (10×10mm²) and indium tin oxide (ITO, 10×50mm²), were cleaned in acetone, ethanol and ultrapure water in succession, and then hydroxylated in a piranha solution (H₂SO₄:H₂O₂=7:3,v/v) at 90°C for 1 h. To maintain electronic conductivity, ITO substrates were only pre-treated in the piranha solution for 15 min at room temperature.

The thickness of multilayer films was measured using spectroscopic ellipsometry (Woollam M-2000DI, USA). The morphology images were obtained with atomic force microscopy Agilent 5500 (USA) using a tapping mode. Raman spectra were obtained from a Renishaw Invia system (UK). Fourier transform infrared spectrum (FTIR) was recorded with a Thermo Nicolet 5700 spectrometer (USA). UV-Vis spectrometer Lambda800 (USA) was used to investigate the self-assembly process. X-ray photoelectron spectroscopy Thermo Escalab 250 (USA) was performed with the element and valence state. All electrochemical measurements were carried out on an electrochemical workstation CHI 660D (Shanghai Chenhua, China) with a three-electrode system in 1 M Na₂SO₄ electrolyte. The Pt sheet worked as the counter electrode and Ag/AgCl as the reference electrode. The working electrodes were ITO assembled with graphene multilayer films.

3. Results and Discussion

With the abundant functional groups, including epoxy, hydroxyl, and carboxyl, GO could be involved in a wide

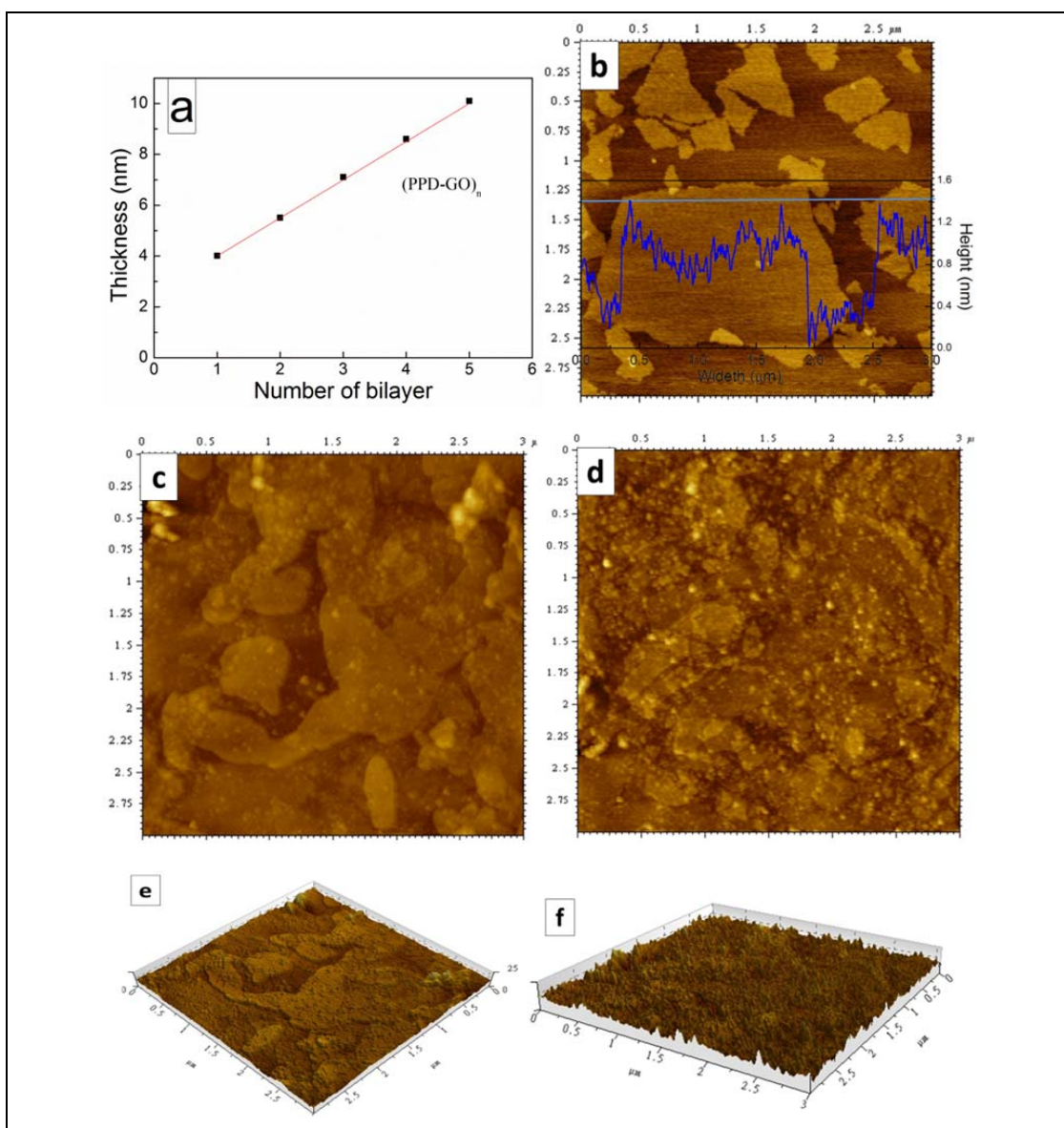


Figure 1. (a) Plots of thickness versus bilayer number for the (PPD-GO)_n; (b) AFM image of GO, (c, d) Morphology and 3D topography (e, f) of GO layers (c, e) and GO-PPD layers (d, f)

range of chemical reactions to realize its multiple functional ability [8, 23, 24]. Here, we utilized the reaction of epoxy and amidogen to assemble graphene layer-by-layer. The formation mechanism is illustrated in scheme 1. Firstly, the aminated substrates were immersed in the GO solution (0.1 mg mL⁻¹) to produce a monolayer of graphene oxide. After ultrasonic washing to remove the absorbed graphene oxide, the composite substrates were dipped in a PPD solution of dimethyl sulfoxide, where PPD was grafted onto the GO surfaces. The substrates were then immersed in the GO solution again to produce the first bilayer of PPD-GO. The (PPD-GO)_n multilayer films were obtained by repeating the previous processes. Finally, the multilayer films were treated by hydrogen iodide vapour to induce the (PPD-GO)_n into (PPD-rGO)_n. As shown in Figure 1a, with the number of the bilayers of PPD and GO increasing,

the thickness of the (PPD-GO)_n (n=1, 2, 3, 4, 5) multilayer film was linearly increased (4.0 nm, 5.5 nm, 7.1 nm, 8.6 nm and 10.1 nm) as the thickness of the first APTES/GO layer was ~2.6 nm. The average increased thickness of the next five PPD-GO layers was ~1.5 nm, the total thickness of GO (~1.0 nm) and a benzene ring (~0.5 nm). With the rigid construct of a benzene ring, the GO layers were separated an interval of 0.5 nm. As a result, these demonstrated successful layer-by-layer assembly with single-layer graphene.

The prepared graphene oxide was tested by atomic force microscopy (AFM). As shown in Figure 1b, the thickness of GO was approximately 1.0 nm. Importantly, the size of GO was about 2.0 μm, which was beneficial for GO assembled layer-by-layer. Figure 1c shows that the GO layers were deposited parallel to the substrates. After being dipped into

the PPD solution, many nano-particles were grown on the surfaces of graphene oxide layers (Figure 1d). Initially the deposited GO film was smooth, while the entire surface later became relatively rough as shown by the 3D geography in Figure 1e and 1f, and many nano-scale spaces between graphene layers were formed. As is well known, the accessible free spaces could allow electrolyte ion storage and circulation.

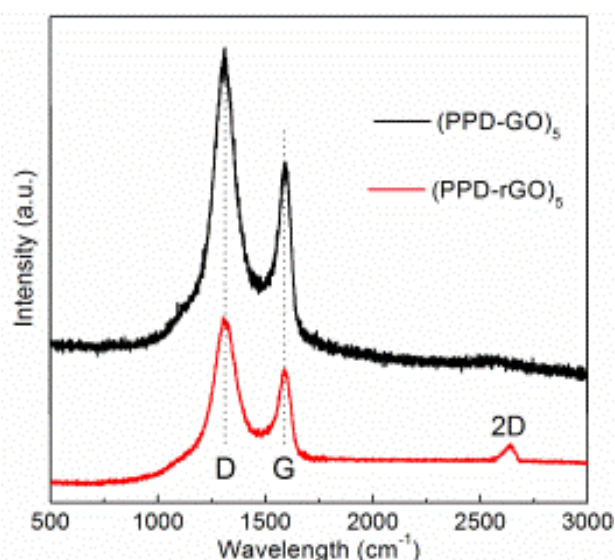


Figure 2. Raman spectra of (PPD-GO)₅ and (PPD-rGO)₅.

The chemical structure of the multilayer film was investigated by the Raman spectrum. Figure 2 presents two prominent peaks at 1321 cm⁻¹ and 1592 cm⁻¹ in the (PPD-GO)₅ and (PPD-rGO)₅, which corresponded to the D band and G band, respectively. The D band represents the defect of sp³-hybridized, while the G band is owed to the in-plane vibration of sp²-hybridized. It could be found that the intensity ratio (I_D/I_G) decreases from 1.52 to 1.28 along the chemical reduction, indicating that (PPD-GO)₅ was successfully reduced to (PPD-rGO)₅. In particular, a small peak at 2690 cm⁻¹, which was attributed to the 2D band, indicated that the existential state of graphene in the multilayer film was a single layer.

To confirm the occurrence of the ring-opening reaction between GO and PPD, FTIR were recorded. Figure 3 shows that the absorption peaks at 880 and 1050 cm⁻¹ were ascribed to the epoxy vibrations in GO. The other characteristic peaks at 1230, 1635, 1730 and 3430 cm⁻¹ indicated that GO owned hydroxyl and carboxyl groups. In the rGO spectrum, all the peaks weakened and new peaks of 1560 and 1214 cm⁻¹ appeared, indicating that GO was successfully reduced to rGO using hydrogen iodide vapour. After reacting with APTES or PPD, the peaks of 880 and 1050 cm⁻¹ could not be observed, and a weak peak at 1098 cm⁻¹ appeared that was ascribed to the generation of C-N. Therefore, it was confirmed that the epoxy groups reacted with the amidogen during the LBL assembly process.

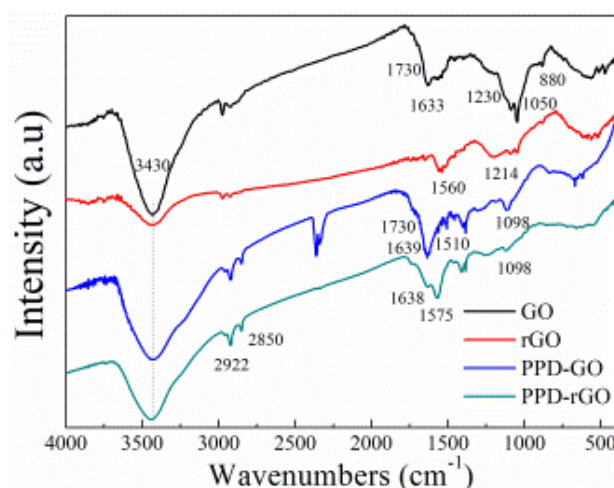


Figure 3. FTIR spectra of GO, rGO, PPD-GO, PPD-rGO

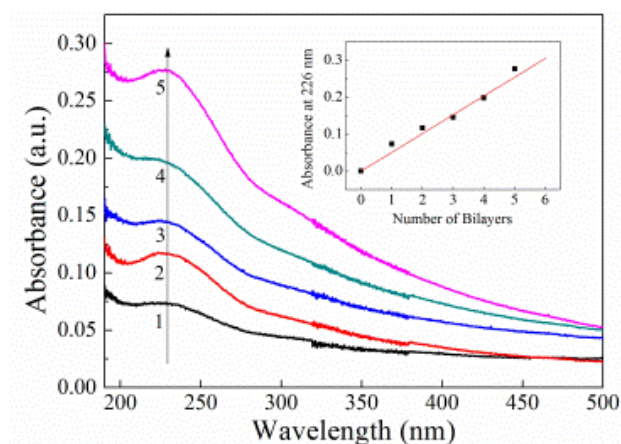


Figure 4. UV-vis spectra of (PPD-GO)_n (n=1,2,3,4,5) multilayer films

Besides, a new weaker peak was detected, which could be explained by the formation of COO-NH₃⁺[25].

UV-vis absorption spectroscopy was used to monitor the assembly process. Figure 4 shows that all of the films displayed an absorption peak at 226 nm owing to the conjugated structure of GO. More importantly the intensity increased nearly linearly, indicating that GO was successfully assembled layer-by-layer and that the assembly process was repeatable. It deserves to be mentioned that the absorption peaks were basically unchanged after ultrasonic treatment for 30 minutes, demonstrating that the structure was steady.

XPS analysis was applied to provide further confirmation of this scheme. The C1s and N1s XPS spectra of ultrathin (PPD-GO)₅ and (PPD-rGO)₅ films are shown in Figure 5. The (PPD-GO)₅ film manifested five signals at 284.6, 285.1, 285.7, 287.1 and 289.1 eV, ascribed to the valence bonds C-C, C-N, C-O, C=O, and C(O)-O, respectively. Additionally, the N1s spectrum displayed signals of 389.9 eV (C-N) and 400.1 eV (C-NH₃⁺). These results demonstrate the reaction of epoxy and amidogen groups. After the (PPD-GO)₅ films were reduced to form (PPD-rGO)₅, the signals at 285.7,

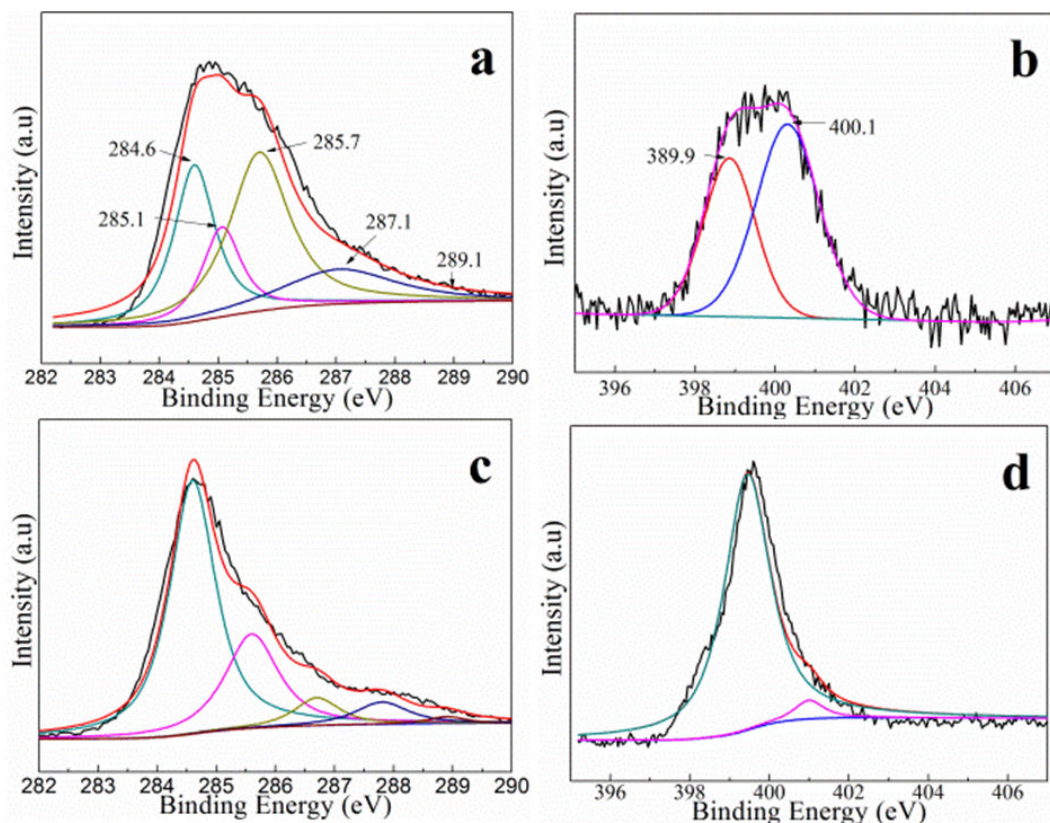


Figure 5. (a) C 1s and (b) N 1s spectra of PPD-GO; (c) C 1s and (d) N 1s spectra of PPD-rGO

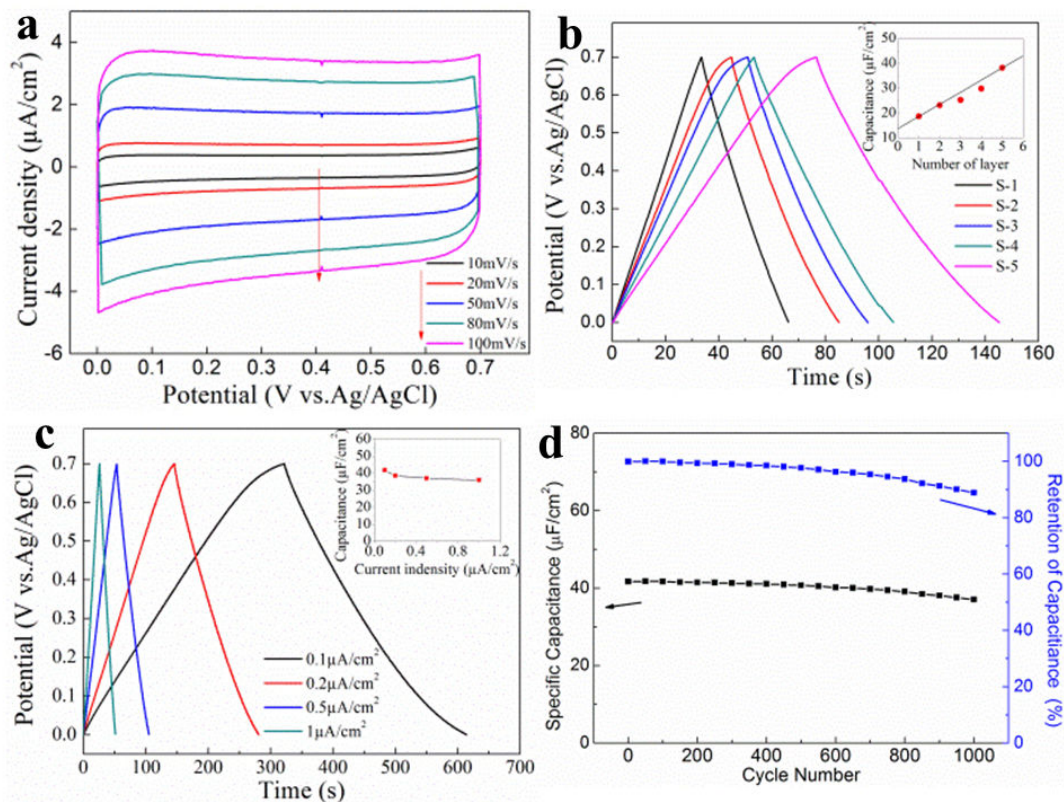


Figure 6. (a) CV curves of (PPD-rGO)₅ electrode at different scanning rates; (b) Charge-discharge curves of (PPD-rGO)₅ electrode at different current densities; (c) Charge-discharge curves of (PPD-rGO)_n (n=1,2,3,4,5) electrodes at a current density of 0.4 $\mu\text{A}/\text{cm}^2$; (d) Cyclic performance of (PPD-rGO)₅ electrode at 0.1 $\mu\text{A}/\text{cm}^2$ for 1000 cycles

287.1 and 289.1 eV weakened, indicating that the content of hydroxyl and carboxyl groups had decreased in accordance with the FTIR spectra.

To explore the potential application in supercapacitors, (PPD-rGO)_n films were assembled on ITO to examine their electrochemical properties. The cyclic voltammetry (CV) curves of (PPD-rGO)₅ are shown in Figure 6a; the nearly rectangular curves, even at a wide range of scanning rates, indicated that the multilayer graphene film possessed a favourable capacitance. The capacitances were ascribed to the combination of a double layer capacitance of graphene and the faradaic pseudocapacitance of PPD. The good charge propagation was ascribed to the spaces for ionic storage between the graphene layers.

The area specific capacitance (C_s , $\mu\text{F}/\text{cm}^2$) is calculated according to the following equation:

$$C_s = \frac{I\Delta t}{\Delta V \times S}$$

where I (μA), Δt (s) and ΔV (V) are the discharge current, discharge time and potential drop in the charge/discharge curve, respectively, and S (cm^2) is the area of the active material. The representative charge-discharge curves of (PPD-rGO)₅ films at different current densities are shown in Figure 6b. The curves show a symmetric triangular shape, which indicated the ideal EDL capacitance of the graphene. The C_s at different current densities decreased slightly, demonstrating that the graphene electrodes had a good rate capability (inset of Figure 6b). The well-designed structure and abundant spaces facilitated ionic circulation. Additionally, electrical conductivity was improved due to the π - π conjugated structure. The charge-discharge curves with different numbers of layers are shown in Figure 6c, displaying that C_s increased almost linearly with the layer number. This result implied the full utilization of each deposited graphene layer.

Cycling stability is another important factor for the practical application of supercapacitors. The (PPD-rGO)₅ electrode showed an excellent cycling stability with 88.9 % of the initial capacitance at $0.1 \mu\text{A}/\text{cm}^2$ after 1000 cycles (Figure 6d). This may be explained by the covalent interactions formed between the epoxy and amidogen, which were steady enough to provide a long lifetime.

4. Conclusions

In summary, a novel type of ultrathin graphene film was prepared via a layer-by-layer self-assembly method. Multilayer films assembled by covalent bonds were reproduced, and the structure was uniform and stable. With the PPD as a covalent cross-linking agent, the multilayer graphene films were assembled into an open morphology with a large layer space; the graphene therefore exhibited highly accessible surface areas. As a result,

the (PPD-rGO)₅ electrode performed an excellent capacitive capacity, good rate capacity and long-term cyclic stability. Finally, we believe that the success of ultrathin graphene multilayer films by the covalent self-assembly method will be useful for supercapacitors.

5. Acknowledgements

This work was supported by the Scientific and Technological Innovation Project of Fujian Province (Grant No. 2012H6008), Scientific and Technological Innovation Project of Fuzhou City (Grant No. 2013-G-92).

6. References

- [1] El-Kady M F, Strong V, Dubin S and Kaner R B (2012) Laser Scribing of High-performance and Flexible Graphene-based Electrochemical Capacitors. *Science* 335:1326-1330.
- [2] Conway B E (1991) Transition from "supercapacitor" to "battery" Behavior in Electrochemical Energy Storage. *Journal of the Electrochemical Society* 138:1539-1548.
- [3] Simon P and Gogotsi Y (2008) Materials for Electrochemical Capacitors. *Nature Materials* 7:845-854.
- [4] Liu X, Shang P, Zhang Y, Wang X, Fan Z, Wang B and Zheng Y (2014) Three-dimensional and Stable Polyaniline-grafted Graphene Hybrid Materials for Supercapacitor Electrodes. *Journal of Materials Chemistry A* 2:15273-15278.
- [5] Chmiola J, Yushin G, Gogotsi Y, Portet C, Simon P and Taberna P L (2006) Anomalous Increase in Carbon Capacitance at Pore Sizes Less than 1 Nanometer. *Science* 313:1760-1763.
- [6] Zhang L L and Zhao X (2009) Carbon-based Materials as Supercapacitor Electrodes. *Chemical Society Reviews* 38:2520-2531.
- [7] Pandolfo A and Hollenkamp A (2006) Carbon Properties and Their Role in Supercapacitors. *Journal of Power Sources* 157:11-27.
- [8] Allen M J, Tung V C and Kaner R B (2009) Honeycomb carbon: A Review of Graphene. *Chemical Reviews* 110:132-145.
- [9] Stoller M D, Park S, Zhu Y, An J and Ruoff R S (2008) Graphene-based Ultracapacitors. *Nano Letters* 8:3498-3502.
- [10] Huang X, Zeng Z, Fan Z, Liu J and Zhang H (2012) Graphene-based Electrodes. *Advanced Materials* 24:5979-6004.
- [11] Xia J, Chen F, Li J and Tao N (2009) Tao Measurement of The Quantum Capacitance of Graphene. *Nature Nanotechnology* 4:505-509.
- [12] Yan J, Liu J, Fan Z, Wei T and Zhang L (2012) High-performance Supercapacitor Electrodes Based on Highly Corrugated Graphene Sheets. *Carbon* 50:2179-2188.

- [13] Wen Z, Wang X, Mao S, Bo Z, Kim H, Cui S, Lu G, Feng X and Chen J (2012) Crumpled Nitrogen-doped Graphene Nanosheets with Ultrahigh Pore Volume for High-performance Supercapacitor. *Advanced Materials* 24:5610-5616.
- [14] Li H, Liu L and Yang F (2013) Covalent Assembly of 3D Graphene/polypyrrole Foams for Oil Spill Cleanup. *Journal of Materials Chemistry A* 1:3446-3453.
- [15] Chang K and Chen W (2011) L-cysteine-assisted Synthesis of Layered MoS₂/graphene Composites with Excellent Electrochemical Performances for Lithium Ion Batteries. *ACS Nano* 5:4720-4728.
- [16] Park J S, Cho S M, Kim W -J, Park J and Yoo P J (2011) Fabrication of Graphene Thin Films Based on Layer-by-layer Self-assembly of Functionalized Graphene Nanosheets. *ACS Applied Materials & Interfaces* 3:360-368.
- [17] Yu B, Liu X, Cong H, Yuan H, Wang D and Li Z (2014) Graphene-Based Multilayers Constructed from Layer-by-Layer Self-Assembly Techniques. *Journal of Nanoscience and Nanotechnology* 14:1145-1153.
- [18] Batra A, Cvetko D, Kladnik G, Adak O, Cardoso C, Ferretti A, Prezzi D, Molinari E, Morgante A and Venkataraman L (2014) Probing the Mechanism for Graphene Nanoribbon Formation on Gold Surfaces through X-ray Spectroscopy. *Chemical Science* 5:4419-4423.
- [19] Matassa R, Orlanducci S, Tamburri E, Guglielmotti V, Sordi D, Terranova M L, Passeri D and Rossi M (2014) Characterization of Carbon Structures Produced by Graphene Self-assembly. *Journal of Applied Crystallography* 47:222-227.
- [20] Zhu J and He J (2012) Assembly and Benign Step-by-step Post-treatment of Oppositely Charged Reduced Graphene Oxides for Transparent Conductive Thin Films with Multiple Applications. *Nanoscale* 4:3558-3566.
- [21] Zhang X, Chen H and Zhang H (2007) Layer-by-layer Assembly: from Conventional to Unconventional Methods. *Chemical Communications* 1395-1405.
- [22] Ou J, Wang J, Liu S, Mu B, Ren J, Wang H and Yang S (2010) Tribology Study of Reduced Graphene Oxide Sheets on Silicon Substrate Synthesized via Covalent Assembly. *Langmuir* 26:15830-15836.
- [23] Zhu Y, James D K and Tour J M (2012) New Routes to Graphene, Graphene Oxide and Their Related Applications. *Advanced Materials* 24:4924-4955.
- [24] Liu J, Tang J and Gooding J J (2012) Strategies for Chemical Modification of Graphene and Applications of Chemically Modified Graphene. *Journal of Materials Chemistry* 22:12435-12452.
- [25] Mo Y, Zhu M and Bai M (2008) Preparation and Nano/microtribological Properties of Perfluorodecanoic Acid (PFDA)-3-aminopropyltriethoxysilane (APS) Self-assembled Dual-layer Film Deposited on Silicon. *Colloids and Surfaces A: Physicochemical and Engineering Aspects* 322:170-176.